

The effect of combined cyclic mechanical stretching and microgrooved surface topography on the behaviour of fibroblasts

WA Loesberg, XF Walboomers, JJWA van Loon and JA Jansen

J Biomed Mater Res A. 75 (3), 723-732, 2005

INTRODUCTION

Previous studies have shown that connective tissue is responsive to mechanical loading. Various *in vitro* systems have been developed to study this phenomenon. One of such systems is based on mechanical loading by uni-axial stress [1; 2]. Under the influence of uni-axial stress, cultured fibroblasts have a tendency to orient themselves. Fibroblasts orientation begins within hours after initiation of stretch, and the cells remain oriented for several hours after cessation of stretch. The alignment is dependent on the cell type used, but in general is perpendicular to the stretch direction [1; 3-10]. Earlier studies have proven that similar cell alignment can also be induced by topographical clues. For instance, fibroblasts cultured on microgrooved culturing substrates align along the grooves [11-16]. Topography can actively direct cell shape, and spreading. The cells are capable of sensing the structural shape of their environment, and determine their form and function appropriately. In both situations, various biological responses have been studied: remodelling of actin cytoskeleton [6; 14; 17; 18], changes in cell proliferation [10; 17; 19-22], and changes in gene expression and protein synthesis [23-27].

It is understood that the cellular response to stretching and microgrooves can interact [5]. Still, numerous parameters have to be investigated to fully understand cell behaviour. Unknown is, whether the observed effects still apply when fibroblast cells are seeded on different microgroove dimensions, as used in the experiments by Brunette and co-workers [15], [28; 29] and by others [19]. These researchers reported favourable tissue responses along certain types of textures, in a range of animal studies. Simultaneous *in vitro* work showed that topographic features affect cellular alignment, direction of proliferation, cellular attachment, growth rate, metabolism, and cytoskeleton arrangement. Therefore, the production of extracellular matrix components of the fibroblasts (collagen type I, fibronectin), and integrins, will also be investigated in this study as to supply additional information.

The aim of this study is therefore to evaluate *in vitro* the differences in cellular behaviour, between fibroblast cells cultured on smooth and microgrooved substrates, which undergo cyclic stretching. Our hypothesis is that cellular shape and orientation is determined by the topographical clues on the substrates. To ensure comparison to previous work two different topographies were used: a 10 µm wide square-groove [30] [31] and a 40 µm wide V-groove [32; 33]. As controls, smooth substrates were used. Onto all substrates rat dermal fibroblasts (RDF) were cultured. After mechanical loading the morphological characteristics were compared using scanning electron microscopy to supply qualitative information on the spreading and orientation. Immuno-staining of filamentous actin was visualised with fluorescence microscopy and cell alignment was scored quantitatively. Finally, the expression of collagen type I, fibronectin, and α1- and β1-integrin were investigated, as the primary molecules involved in cell-matrix adhesion.

MATERIALS AND METHODS

Substrates:

Silicone dishes were produced by mixing two-component polydimethylsiloxane (PMDS) Elastosil 601A en 601B (Wacker Chemie, Riemerling, Germany) in a ratio of 10:1. The silicone mixture was poured into an acrylic dish-mold. The mixture was left for one hour for air bubbles to escape, after which the mold was placed in an oven for 2 hours at 50 °C.

Microtextured patterns were photo-etched in a silicon wafer using lithographic and reactive ion etching techniques as described by Walboomers et al [11]. **Figure 1** shows the two different topographies which were used in this study: a 10 µm wide groove/ridge, 1 µm deep (square-groove) and a 40 µm wide groove, 5 µm wide ridge and 30 µm deep (V-groove). These silicon wafers were used as templates for the production of silicone culturing substrates. After mixing of the two components, pouring, and curing of the silicone, the silicone replicas were removed from

the template. The obtained silicone substrates were bonded to the bottoms of the silicone dishes described above, using room temperature vulcanising (RTV) silicone adhesive (Nusil Technology, Carpinteria, CA, USA). The grooved substrates were attached either parallel or perpendicular to the stretching direction (**Figure 2**). Smooth silicone substrates were prepared to serve as the control group. Subsequently, all dishes were washed in a 10% solution of Liqui-Nox Detergent (Alconox Inc., New York, NY, USA), sonicated in a 1% Liqui-Nox solution, rinsed extensively in MilliQ-water, and autoclaved for 15 min at 121 °C. Just before cell culture, a radio frequency glow-discharge (RFGD) treatment was applied for 10 min at a pressure of 2.0×10^{-2} mbar (Harrick Scientific Corp., Ossining, NY, USA) to promote cell attachment by improving the wettability of the substrates [34-38].

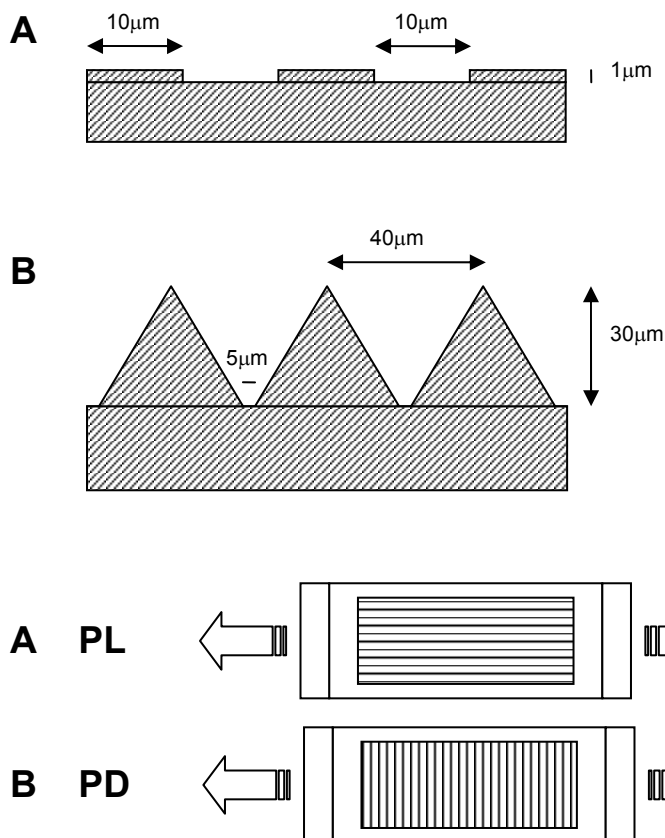


Figure 1: Graphical presentation of a cross section of template surface topographies used in this study: (A) 10 μm square groove, and (B) V-groove topography; here the wall and floor of the groove meet at angle of 120°. For clarity the drawings are not to scale.

Figure 2: Silicone dishes with microgrooved substrates attached on the bottom. (A) Grooves parallel (PL), and (B) perpendicular (PD) to the stretching direction. The culture area of the microgrooved surfaces is 3 x 6 cm.

Cell culture:

RDFs were obtained from the ventral skin of male Wistar rats [39]. To ensure quick and constant availability, cells were cryo-preserved. Before experimentation, cells were thawed and cultured in α -Modified Eagles Medium (α -MEM) containing Earle's salts, L-glutamine, 10% foetal calf serum (FCS), and gentamicin (50 $\mu\text{g}/\text{ml}$). Cells were cultured in a CO₂ incubator set at 37 °C in a humidified atmosphere. Experiments were performed with 6 - 8th culture generation cells. Onto all substrates, 1×10^4 cells/cm² were seeded. After incubation of 1 h, the silicone dishes were placed inside a custom-made stretching apparatus (**Figure 3**), as described previously [1; 3; 40; 41]. Different cyclic stretching magnitudes were applied: 0%, 4%, 8% at a 1 Hz frequency. Also, two different stretch durations were applied: 3 or 24h. Directly at the end of each experimental run, the RDF cell layers were washed three times with PBS and prepared for further analysis.

Scanning electron microscopy:

To assess cellular morphology of the fibroblasts, Scanning electron microscopy (SEM) was used. Directly after stretching, cells were fixed for 5 minutes in 2% glutaraldehyde, rinsed for 5 minutes

with 0.1 M sodium-cacodylate buffer (pH 7.4), dehydrated in a graded series of ethanol, and dried in tetramethylsilane to air. The specimens were sputter-coated with gold and examined and photographed using a Jeol 6310 SEM.

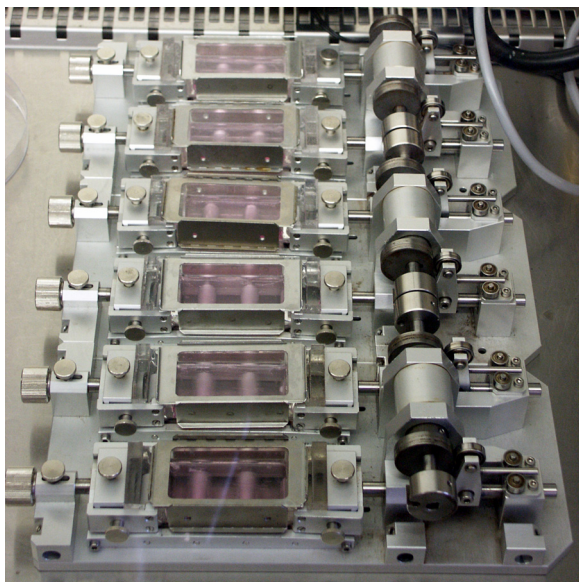


Figure 3: The stretching device that was used to apply a uniform cyclic strain of 4 or 8 % at 1 Hz for several hours.

Immunofluorescence

To observe the cytoskeleton, cells were fixed for 30 minutes in 2% paraformaldehyde, and permeabilised with 1% Triton X100 for 5 min. Then filamentous actin was stained with Alexa Fluor 568 phalloidin (Molecular Probes Inc., Eugene, OR, USA) diluted in PBS containing 1% Bovine Serum Albumin (BSA) to block non-specific epitopes, according to manufacturers specifications. Finally, the specimens were examined with a Leica/Leitz DM RBE Microscope system at magnification of 10x. Cytoskeletal components were examined for their overall morphology as well as their orientation with respect to the groove direction as described below.

Image Analysis

The fluorescence micrographs were analyzed with Scion Image software (Beta Version 4.0.2, Scion Corp., Frederick, MY, USA). The orientation/distribution of the entire cell was examined. For each sample four fields were selected randomly. Within each field two criteria were used for cell selection: (1) the cell is not in contact with other cells and (2) cell is not in contact with the field perimeter. Thereafter, on each cell within the field the following parameters were examined: first, the maximum cell diameter was measured as the longest distance between two edges within the cell borders. Second, the angle between this axis and the grooves (or an arbitrarily selected line for smooth surfaces). This latter measurement will be termed the orientation angle. Using Clarks criteria [42], cells oriented at 0–10 degrees from the groove direction were regarded to be aligned.

RT-PCR analysis

Total RNA was isolated from the RDFs with a RNA isolation and stabilisation kit (QIAGEN, Hilden, Germany), and cDNA was synthesised from 1 mg of total RNA. After an initial denaturation for 2 min at 95°C, the samples were amplified for 35 cycles, consisting of annealing at 55 °C for 1 min, elongation at 72 °C for 2 min, and denaturation at 95 °C for 1 min. The duration of the final elongation reaction was increased to 10 min at 72 °C to permit completion of reaction products. The PCR products were separated on a 1.5% (w/v) agarose gel, and visualised by ethidium bromide staining. Semi-quantitative analysis of band intensity was performed using Quantity One 1-D analysis software for Windows (Version 4.5.0, Bio Rad, Hercules, California,

USA). The RT-PCR products value corresponding to collagen type I (only 24 hours samples), fibronectin, α 1 integrin, β 1 integrin were divided by glyceraldehyde-3-phosphate dehydrogenase (GAPDH) value. The forward and reverse primer sequence can be found in **Table 1**.

	5' Primer (Forward)	3'Primer (Reverse)	Size (bp)
Collagen Type I	TGTTCGTGGTTCTCAGGGTAG	TTGTCGTAGCAGGGTTCTTC	254
Fibronectin	CCTTAAGCCTCTGCTCTGG	CGGCAAAAGAAAGCAGAACT	301
α 1-Integrin	AGCTGGACATAGTCATCGTC	AGTTGTCATGCGATTCTCCG	374
β 1-Integrin	AATGTTTCAGTGCAGAGCC	TTGGGATGATGTCGGGAC	262
GAPDH	CGATGCTGGCGCTGAGTAC	CGTTCAGCTCAGGGATGACC	470

Table 1: Forward and reverse primer sequences used in this study.

Statistical analysis:

Acquired quantitative data were analysed using SPSS for Windows (Release 12.0.1, SPSS Inc., Chicago, USA). The effects of and the interaction between both time or force and surface were analysed using two-way analysis of variance (ANOVA). A probability (p) value less than or equal to 0.05 was considered significant.

RESULTS

Scanning Electron Microscopy

SEM revealed that the pattern of grooves and ridges were perfectly reproduced in the silicone rubber substrata (**Figure 4**). As observed earlier by Walboomers et al. [11], the ridges appear to have an additional roughness due to the etching process, which is used to fabricate the original silicon wafers. This roughness also was faithfully replicated onto the silicone substrata, indicating the accuracy of the casting process.

When analysing cell morphology, SEM showed that the RDF cells aligned along the groove direction on all grooved surfaces. On the smooth substrata (control) cells were spread out in a random fashion. Cells cultured on the substrates with the more pronounced grooves (V-groove substrate) seemed to be more clearly aligned than compared to square-groove substrates. The same applied for cells cultured for the longer time period (24h) in comparison to the 3h culturing. The cells cultured on square-groove substrate have a flat appearance and were able to descend into the grooves, whereas the cells cultured on V-groove substrate were nearly always found on top of the ridges. Their cell bodies frequently crossed over to the adjacent ridge, forming a bridge between them.

Fluorescence microscopy and Image Analysis

Fluorescence microscopy clearly showed the actin filaments stained with phalloidin-TRITC (**Figure 5**). Subsequent image analysis confirmed the cellular behaviour, as seen under the SEM, i.e. while the RDFs cultured on grooved substrates in general show alignment along the grooves; the smooth control samples do not induce any form of alignment. The quantified results for cell alignment are presented as box-whisker plots (**Figure 6**). Such a graph shows the distribution midpoint, the first and third quartile (boxes), and the largest and smallest observation (whiskers). The effects of the main parameters are expressed as an alignment percentage of the total number of cells, and are displayed in **Table 2**. Due to poor sample recovery no data was available for groups S3H8, PDSQ3H4, and PLV24H0.

An ANOVA was performed on the data, for all main parameters: groove type, groove orientation, stretch force, and time. In this analysis, all parameters proved significant, except stretch force. Regarding groove type 82% of the cells were aligned along the V-grooves, combined with prolonged culture time, and 76% of the cells in square grooves, compared to 19% of the smooth substrates.

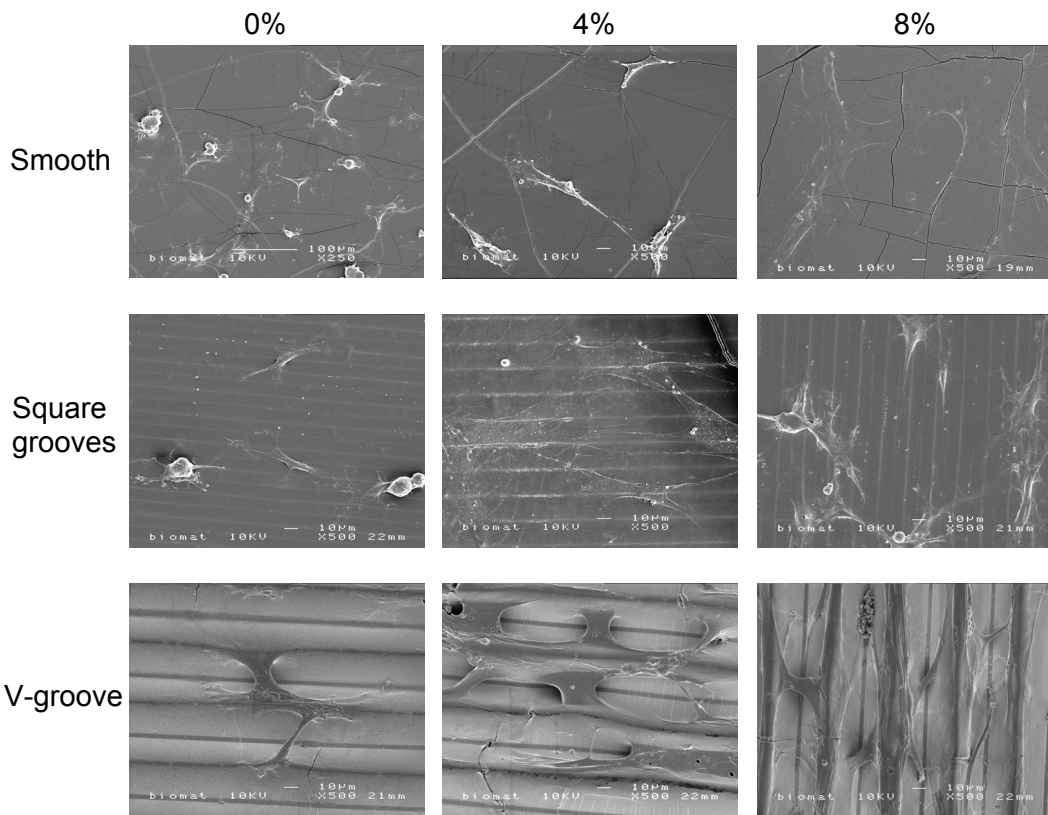


Figure 4: SEM micrographs of RDFS cultured under various circumstances. Top row: smooth substrates, 0% stretch force (left), 4% stretch force (centre), and 8% stretch force (left). Middle row: square-groove substrates, 0% parallel (left), 8% parallel (centre), 8% perpendicular (right). Bottom row: V-groove substrates, 0% parallel (left), 8% parallel (centre), 8% perpendicular (right). All micrographs were taken from 24 hrs samples.

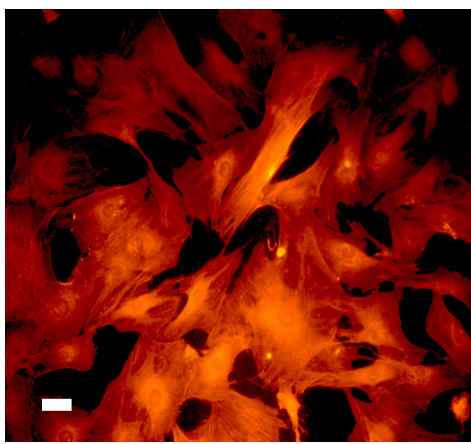


Figure 5: Phalloidin-TRITC fluorescence staining of the actin filaments of rat dermal fibroblasts cultured on a smooth silicone substrate. Magnification x20. Bar size = 10 micron.

With regard to groove direction; microgrooves perpendicular to the stretch direction elicit a better alignment: 82% of the cells aligned on perpendicular orientation compared to 57% on parallel orientation on V-grooves. On square grooves the percentages increased from 36% (parallel) to 77% (perpendicular).

The amount of stretching force does not influence cell alignment along the grooved topography. The effect of stretch force from 0% to 4%, or from 4% to 8% is marginal. The percentages of aligned cells are close to each other, average percentage differences are about 3-5%.

Finally, the effect of time on the alignment percentage is minimal, but significant. 24 hour samples show a higher alignment compared to their 3 hour counterparts; in smooth samples there is a 4% increase in time, on V-grooves and square-grooves this is 9% and 22% respectively. It should be noted that interaction of the parameters groove type and groove orientation makes exact interpretation difficult.

<i>Degree subgroups</i>	<i>0 - 10</i>	<i>11 - 45</i>	<i>46-90</i>
<i>Sample group</i>			
PLSQ3H0	35.4	39.8	24.8
PLSQ24H0	47.8	40.7	11.5
PDSQ3H0	38.0	44.8	17.2
PDSQ24H0	57.4	38.0	4.6
PLV3H0	66.9	27.4	5.7
PLV24H0	n/a	n/a	n/a
PDV3H0	75.7	21.8	2.5
PDV24H0	85.0	15.0	0
PLSQ3H4	23.8	39.1	37.1
PLSQ24H4	31.1	44.8	24.1
PDSQ3H4	n/a	n/a	n/a
PDSQ24H4	59.9	35.7	4.4
PLV3H4	53.5	37.8	8.7
PLV24H4	80.3	17.6	2.1
PDV3H4	76.9	18.5	4.6
PDV24H4	89.3	10.0	0.7
PLSQ3H8	14.9	32.2	52.9
PLSQ24H8	34.3	33.4	32.3
PDSQ3H8	58.6	34.7	6.7
PDSQ24H8	61.7	38.1	3.2
PLV3H8	55.7	31.6	12.7
PLV24H8	79.4	17.1	3.5
PDV3H8	72.5	23.4	4.1
PDV24H8	77.6	16.3	6.1
S3H0	15.3	34.8	49.9
S24H0	15.3	40.9	43.8
S3H4	16.8	49.0	34.2
S24H4	24.2	51.6	24.2
S3H8	n/a	n/a	n/a
S24H8	25.0	52.4	22.6

Table 2: Percentages of aligned cells divided in three subgroups. See Figure 6 for explanation of abbreviations.

RT-PCR

The mRNA expression for $\alpha 1$ -, and $\beta 1$ -integrins, fibronectin, and collagen type I of the RDF cells was examined after each experimental run. An example of the visualised samples, separated on agarose gel, can be found in **Figure 7**, while all RT-PCR sample product ratios are listed in **Table 3**. With respect to the grooved samples; $\beta 1$ levels in the 0% stretch force were lower than those in the stretched samples. The Collagen Type I levels increased with higher stretch force. The smooth control samples showed that most product values were equal to the household gene, except the $\beta 1$ -integrin subunit in samples experiencing either 4% or 8%, stretch force. Also the $\alpha 1$ -integrin subunit decreased with higher stretch magnitude.

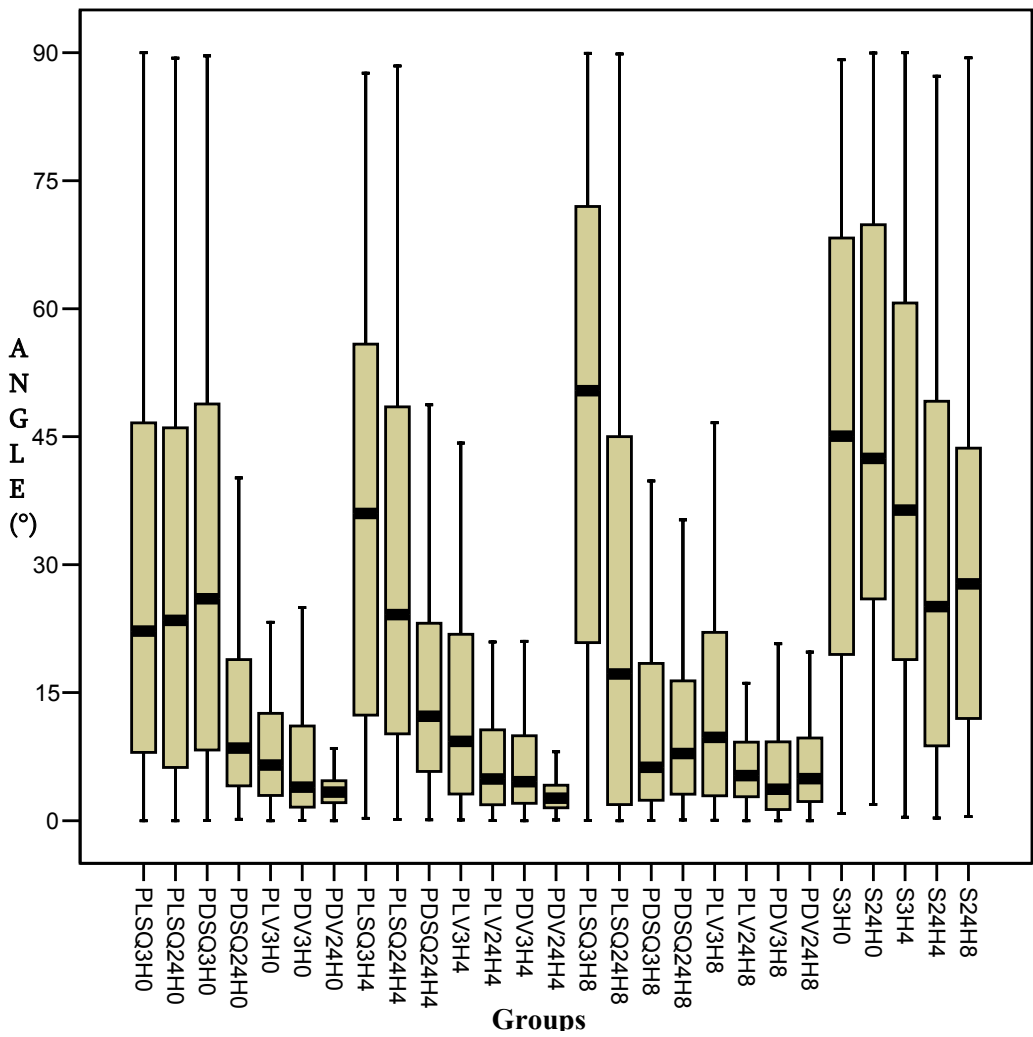


Figure 6: Box-whisker plot showing the distribution of cellular orientation. Note that no orientation is observed on the smooth samples and that orientation on grooved samples is dependent on the groove type. PL = parallel, PD = perpendicular, SQ = square groove, V = V-groove, 3H and 24H stands for the experiment time, and 0, 4, and 8 stands for the applied stretch force. For each parameter at least 300 individual cells were analysed.

DISCUSSION

The aim of this study was to evaluate *in vitro* the differences in cellular behaviour, between fibroblast cells, cultured on smooth and microgrooved substrates, which undergo cyclic stretching. From our data it could be concluded that independent of the stretch magnitude or whether the microgrooves are oriented parallel or perpendicular to the stretching direction, the fibroblasts primarily adjust their shape according to substrate surface (micro) features, whilst a secondary role is played by mechanical loading.

Scanning electron microscopy, immunofluorescence staining, and subsequent image analysis all confirmed that fibroblasts were oriented on both types of microgrooved surfaces. The shapes of the groove surfaces were based on earlier studies. Although the exact confirmation of the grooves differed, the rate of cellular orientation mainly was determined by increasing groove depth. This is in accordance with earlier work of Clark et al. [42; 43]. There it was concluded that groove depth is much more important in alignment of cells than the spacing of the grooves. Even when patterns of nanometer scale were used, an increase in groove depth led to better orientation [16].

Group	PL	PL	PD	PD	PL	PL	PD	PD	PL	PL	PD	PD	PL	PL	PD	PD
	SQ	SQ	SQ	SQ	V	V	V	V	SQ	SQ	SQ	SQ	V	V	V	V
	3H	24H	3H	24H	3H	24H	3H	24H	3H	24H	3H	24H	3H	24H	3H	24H
	0	0	0	0	0	0	0	0	4	4	4	4	4	4	4	4
$\alpha 1$	0.87	0.98	n/a	0.91	1	1	0.84	0.78	0.90	0.98	1	0.96	1	n/a	1	1
$\beta 1$	0.43	0.51	n/a	0.55	0.33	0.18	0.21	0.36	0.58	0.63	0.71	0.49	0.79	n/a	0.65	0.75
Fibro	0.88	0.61	n/a	0.98	0.80	0.86	0.94	0.67	0.99	1	0.40	1	1	n/a	0.99	0.99
Coll I	n/a	0.61	n/a	0.57	n/a	0.58	n/a	0.58	n/a	0.76	n/a	0.78	n/a	n/a	n/a	0.94

n/a: not available

Group	PL	PL	PD	PD	PL	PL	PD	PD	S	S	S	S	S	S	S	S
	SQ	SQ	SQ	SQ	V	V	V	V	3H	24H	3H	24H	3H	24H	3H	24H
	3H	24H	3H	24H	3H	24H	3H	24H	0	0	4	4	8	8	8	8
	8	8	8	8	8	8	8	8								
$\alpha 1$	1	0.95	n/a	n/a	1	0.3	0.42	1	1	1	1	0.28	1	0.76		
$\beta 1$	1	0.96	n/a	n/a	1	0.91	0.58	0.78	1	1	1	1	0.86	0.84	0.72	
Fibro	1	1	n/a	n/a	1	0.92	1	1	1	1	1	1	1	1	1	
Coll I	n/a	0.96	n/a	n/a	n/a	0.87	n/a	0.99	n/a	1	n/a	0.96	n/a	1		

Table 3: RT-PCR semiquantitative analysis. Displayed are the ratios between the gene of interest and the household gene GAPDH. See Figure 6 for explanation of group abbreviations.

In the current study, it was seen that cells on square-groove substrates were able to reach the bottom of the 1 μ m deep grooves, whereas on the substrates with V-grooves the cells lost contact with the bottom of the grooves. The cellular extensions probing the V-groove substrate surface only find the top ridge, resulting in extension of the cellular body along these ridges. This difference in behaviour might explain the variation in the orientation between the different groove depths. Orientation is almost independent of groove spacing. There is only a small dependency, probably caused by the fact that sometimes cells cross-over to other top ridges, where part of the cell is extending in the same direction.

In our study, after 3 hours of stretch cellular orientation starts to commence, and after 24 hours the cells have aligned themselves almost entirely along the grooves. This observation was also noted by Neidlinger-Wilke and co-workers [3], studying only the exposure to cyclic stretch (i.e. no surface texturing was applied). These researchers found that the degree of cell alignment continued to improve up to 24 hours. Similarly, Walboomers *et al* [18] described early events displayed by fibroblast cells on textured surfaces. In that particular study, it was found that cell orientation on microtextures starts with the formation of abundant membrane extensions. These are probable signs of exploration and probing of the surface by the cells. Since the cell is lacking

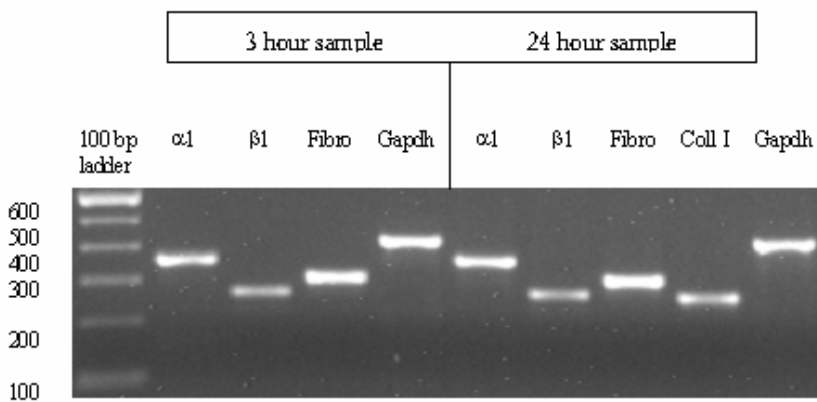


Figure 7: RT-PCR sample example of parallel oriented square-type grooves with 4% stretch force, visualised on agarose gel.

natural ECM, and neighbouring cells, these extensions are formed in all directions. Within hours, the presence of suitable attachment sites is confirmed and contacts are established with deposited ECM material. The cell flattens and spreads, and active filaments form longitudinal stress fibres

[44]. In this study, it was evident that cellular orientation occurred immediately during the cell spreading, and always was parallel to the grooves.

Cell movements or orientation as reaction to mechanical stress might be based on a comparable mechanisms. But in contrast to the responses to microtextures as described above, the reaction towards the mechanical loading can only occur after cell has attached and spread out over the surface, and after the cell has established an inter-connective system of ECM, integrins, and cytoskeleton. From our RT-PCR results it is clear that the production of these components is vital for cells, so they have a mechanically resistant attachment support. This is indicated by the fact that cells under mechanical stimulation show enhanced β 1-integrin and collagen-I levels. The cell-matrix interactions in cultured fibroblasts cells are almost solely mediated via receptors of the integrin family. Upon recognition of the extracellular ligand, integrins start to cluster and become activated, which results in recruitment of an array of proteins and the formation of the focal adhesion complex (FAC), containing both cytoskeletal and signalling molecules [44-47]. Activation results in repeated (de)polymerisation series of actin, and finally the formation of stress fibres. These structures establish a physical link between the ECM components and the cytoskeleton via the integrins, thereby offering a continuous path acting as a mechanotransducer. This “mechanosensing connection” is used by the cells to perform their mechanical functions as for instance the orientation changes as response to the stretching. *In vitro*, cells are geared towards a mechanical equilibrium between the tension of the ECM support and the stress in the cells, since application of external tension or relaxation to the support is rapidly compensated by cell relaxation or traction [45; 46].

From the image analysis it also became clear that substrates with microgrooves perpendicular to the stretch direction elicit a better cell alignment. This is to be expected, since cells align along the grooves, and their orientation is increased by turning away from the stretch direction. This is a new finding, as Wang et al [5] recently reported that cyclic stretching of fibroblasts on microgrooved surfaces did not result in changes of alignment regardless of the stretching direction. In contrast, in our study we did see an additional effect of stretch vs. orientation. Probably, if grooves are made small enough, there is a point where mechanical loading can overrule clues delivered to the cells in the form of surface texturing. However, further research will be required to establish such a threshold dimension for the grooves, as it will necessitate the development of textures at a nanometer level. Such development is currently underway [48]. Several research groups did describe the effects of nanotopography, like Wojciak-Stothard *et al*[7] who used microfabricated grooves and steps, 30-282 nm deep. Teixeira *et al* [49; 50] used grooves with varying pitches between 400 nm and 4 μ m, which were either 150 or 600 nm deep. Still, true nanotechnology to achieve 1-20 nanometer patterns simultaneously in groove width, spacing, and depth, needs to be developed yet.

Some of the issues that remain to be investigated are, whether the cytoskeleton or the cell responses to environmental stimuli occur earlier. Cell orientation should be considered separate from orientation of e.g. actin microfilaments. Shirinsky and co-workers [51] observed that actin cytoskeleton is closely involved in the orientation process, yet when the orientation is completed, the cells are no longer dependent upon that system to maintain their position. Moreover, the relationship between the cytoskeleton and the intracellular signalling is a field in which further research has to be conducted. It is known that the cytoskeleton is constantly remodelling to provide a rapid reaction system for the cell to respond to changes in their mechanical environment, and to supply the best possible way to maintain equilibrium with their environment. For understanding cell reactions, we first need to understand when the reaction is initiated, and in what cell parts: i.e. the focal adhesion complex with its membrane receptors, the cytoskeletal components, or the interacting proteins of the cellular signalling.

CONCLUSION

We can maintain our hypothesis, as microgrooved topography is most effective in applying strains relative to the long axis of the cell. Actin microfilament rearrangement may predetermine the subsequent alignment and elongation of the fibroblasts, which in turn can regulate fibroblast attachment via the intracellular signalling pathways to the underlying membrane receptors. It is here that the secondary effects of stretch force take place. How the mechanotransduction, responsible for the cell orientation, actually works remains to be fully solved. The different forces of uni-axial cyclic stretching combined with the two different loading conditions with respect to the cells long axes may activate different mechano-transduction mechanisms, but the net result is the same: i.e. reduction of mechanical resistance on the cells. The cell will choose the path of least resistance, and adjust its shape to the strongest environmental clue.

REFERENCES

1. Neidlinger-Wilke, C., Grood, E. S., Wang JH-C, Brand, R. A., and Claes, L. Cell alignment is induced by cyclic changes in cell length: studies of cells grown in cyclically stretched substrates. *J Orthop Res* 2001, 286-93, 2001.
2. Winter, L. C., Walboomers, X. F., Bumgardner, J. D., and Jansen, J. A. Intermittent versus continuous stretching effects on osteoblast-like cells in vitro. *J Biomed Mater Res* 2003, 1269-75, 2003.
3. Neidlinger-Wilke, C., Grood, E., Claes, L., and Brand, R. Fibroblast orientation to stretch begins within three hours. *J Orthop Res* 2002, 953-6, 2002.
4. Wang, J. H., Jia, F., Gilbert, T. W., and Woo, S. L. Cell orientation determines the alignment of cell-produced collagenous matrix. *J Biomech* 2003, 97-102, 2003.
5. Wang, J. H., Yang, G., Li, Z., and Shen, W. Fibroblasts responses to cyclic mechanical stretching depend on cell orientation to the stretching direction. *J Biomech* 2003, 573-6, 2003.
6. Pender, N. and McCulloch, C. A. Quantitation of actin polymerization in two human fibroblast sub-types responding to mechanical stretching. *J Cell Sci* 1991, 187-93, 1991.
7. Wojciak-Stothard, B., Curtis, A., Monaghan, W., MacDonald, K., and Wilkinson, C. Guidance and activation of murine macrophages by nanometric scale topography. *Exp Cell Res* 1996, 426-35, 1996.
8. Wojciak-Stothard, B., Madeja, Z., Korohoda, W., Curtis, A., and Wilkinson, C. Activation of macrophage-like cells by multiple grooved substrata. Topographical control of cell behaviour. *Cell Biol Int* 1995, 485-90, 1995.
9. den Braber, E. T., Jansen, H. V., de Boer, M. J., Croes, H. J., Elwenspoek, M., Ginsel, L. A., and Jansen, J. A. Scanning electron microscopic, transmission electron microscopic, and confocal laser scanning microscopic observation of fibroblasts cultured on microgrooved surfaces of bulk titanium substrata. *J Biomed Mater Res* 1998, 425-33, 1998.
10. den Braber, E. T., de Ruijter, J. E., Smits, H. T., Ginsel, L. A., von Recum, A. F., and Jansen, J. A. Quantitative analysis of cell proliferation and orientation on substrata with uniform parallel surface micro-grooves. *Biomaterials* 1996, 1093-9, 1996.
11. Walboomers, X. F., Croes, H. J., Ginsel, L. A., and Jansen, J. A. Growth behavior of fibroblasts on microgrooved polystyrene. *Biomaterials* 1998, 1861-1868, 1998.
12. Walboomers, X. F., Monaghan, W., Curtis, A. S., and Jansen, J. A. Attachment of fibroblasts on smooth and microgrooved polystyrene. *J Biomed Mater Res* 1999, 212-20, 1999.
13. Clark, P., Connolly, P., and Moores, G. R. Cell guidance by micropatterned adhesiveness in vitro. *J Cell Sci* 1992, 287-92, 1992.

14. Oakley, C., Jaeger, N. A., and Brunette, D. M. Sensitivity of fibroblasts and their cytoskeletons to substratum topographies: topographic guidance and topographic compensation by micromachined grooves of different dimensions. *Exp Cell Res* 1997, 413-24, 1997.
15. Brunette, D. M. Fibroblasts on micromachined substrata orient hierarchically to grooves of different dimensions. *Exp Cell Res* 1986, 11-26, 1986.
16. Clark, P., Connolly, P., Curtis, A. S., Dow, J. A., and Wilkinson, C. D. Cell guidance by ultrafine topography in vitro. *J Cell Sci* 1991, 73-7, 1991.
17. Matsuzaka, K., Walboomers, F., de Ruijter, A., and Jansen, J. A. Effect of microgrooved poly-L-lactic (PLA) surfaces on proliferation, cytoskeletal organization, and mineralized matrix formation of rat bone marrow cells. *Clin Oral Implants Res* 2000, 325-33, 2000.
18. Walboomers, X. F., Ginsel, L. A., and Jansen, J. A. Early spreading events of fibroblasts on microgrooved substrates. *J Biomed Mater Res* 2000, 529-534, 2000.
19. von Recum, A. F. and van Kooten, T. G. The influence of micro-topography on cellular response and the implications for silicone implants. *J Biomater Sci Polym Ed* 1995, 181-98, 1995.
20. Neidlinger-Wilke, C., Wilke, H. J., and Claes, L. Cyclic stretching of human osteoblasts affects proliferation and metabolism: a new experimental method and its application. *J Orthop Res* 1994, 70-8, 1994.
21. Buckley, M. J., Banes, A. J., Levin, L. G., Sumpio, B. E., Sato, M., Jordan, R., Gilbert, J., Link, G. W., and Tran Son Tay, R. Osteoblasts increase their rate of division and align in response to cyclic, mechanical tension in vitro. *Bone Miner* 1988, 225-36, 1988.
22. Yoshinari, M., Matsuzaka, K., Inoue, T., Oda, Y., and Shimono, M. Effects of multigrooved surfaces on fibroblast behavior. *J Biomed Mater Res* 2003, 359-368, 2003.
23. Hughes-Fulford, M. and Gilbertson, V. Osteoblast fibronectin mRNA, protein synthesis, and matrix are unchanged after exposure to microgravity. *FASEB J* 1999, S121-7, 1999.
24. Chiquet, M., Renedo, A. S., Huber, F., and Fluck, M. How do fibroblasts translate mechanical signals into changes in extracellular matrix production? *Matrix Biol* 2003, 73-80, 2003.
25. Leung, D. Y., Glagov, S., and Mathews, M. B. Cyclic stretching stimulates synthesis of matrix components by arterial smooth muscle cells in vitro. *Science* 1976, 475-7, 1976.
26. Carver, W., Nagpal, M. L., Nachtigal, M., Borg, T. K., and Terracio, L. Collagen expression in mechanically stimulated cardiac fibroblasts. *Circ Res* 1991, 116-22, 1991.
27. Kessler, J. O. The internal dynamics of slowly rotating biological systems. *ASGSB Bull* 1992, 11-21, 1992.
28. Brunette, D. M. and Chehroudi, B. The effects of the surface topography of micromachined titanium substrata on cell behavior in vitro and in vivo. *J Biomech Eng* 1999, 49-57, 1999.
29. Chehroudi, B., Gould, T. R., and Brunette, D. M. Effects of a grooved epoxy substratum on epithelial cell behavior in vitro and in vivo. *J Biomed Mater Res* 1988, 459-73, 1988.
30. Matsuzaka, K., Walboomers, X. F., Yoshinari, M., Inoue, T., and Jansen, J. A. The attachment and growth behavior of osteoblast-like cells on microtextured surfaces. *Biomaterials* 2003, 2711-9, 2003.
31. Parker, J. A., Walboomers, X. F., Von den Hoff, J. W., Maltha, J. C., and Jansen, J. A. Soft-tissue response to silicone and poly-L-lactic acid implants with a periodic or random surface micropattern. *J Biomed Mater Res* 2002, 91-8, 2002.
32. Chehroudi, B. and Brunette, D. M. Subcutaneous microfabricated surfaces inhibit epithelial recession and

promote long-term survival of percutaneous implants. *Biomaterials* 2002, 229-37, 2002.

33. Chehroudi, B., McDonnell, D., and Brunette, D. M. The effects of micromachined surfaces on formation of bonelike tissue on subcutaneous implants as assessed by radiography and computer image processing. *J Biomed Mater Res* 1997, 279-90, 1997.
34. Walboomers, X. F., Croes, H. J., Ginsel, L. A., and Jansen, J. A. Contact guidance of rat fibroblasts on various implant materials. *J Biomed Mater Res* 1999, 204-12, 1999.
35. den Braber, E. T., de Ruijter, J. E., Ginsel, L. A., von Recum, A. F., and Jansen, J. A. Quantitative analysis of fibroblast morphology on microgrooved surfaces with various groove and ridge dimensions. *Biomaterials* 1996, 2037-44, 1996.
36. Parker, J. A., Walboomers, X. F., Von den, H. J., Maltha, J. C., and Jansen, J. A. Soft tissue response to microtextured silicone and poly-L-lactic acid implants: fibronectin pre-coating vs. radio-frequency glow discharge treatment. *Biomaterials* 2002, 3545-53, 2002.
37. Beumer, G. J., Van Blitterswijk, C. A., and Ponec, M. The use of gas plasma treatment to improve the cell-substrate properties of a skin substitute made of poly(ether)/poly(ester) copolymers. *J Mat Sc Mat Med* 5, 1-6, 94.
38. Amstein, C. F. and Hartman, P. A. Adaptation of plastic surfaces for tissue culture by glow discharge. *J Clin Microbiol* 1975, 46-54, 1975.
39. Freshney, R. I. Culture of animal cells: a multimedia guide. 99. Chichester, John Wiley & Sons Ltd.
40. Wang, H., Ip, W., Boissy, R., and Grood, E. S. Cell orientation response to cyclically deformed substrates: experimental validation of a cell model. *J Biomech* 1995, 1543-52, 1995.
41. Walboomers, X. F., Habraken, W. J., Feddes, B., Winter, L. C., Bumgardner, J. D., and Jansen, J. A. Stretch-mediated responses of osteoblast-like cells cultured on titanium-coated substrates in vitro. *J Biomed Mater Res* 2004, 131-9, 2004.
42. Clark, P., Connolly, P., Curtis, A. S., Dow, J. A., and Wilkinson, C. D. Topographical control of cell behaviour. I. Simple step cues. *Development* 1987, 439-448, 1987.
43. Clark, P., Connolly, P., Curtis, A. S., Dow, J. A., and Wilkinson, C. D. Topographical control of cell behaviour: II. Multiple grooved substrata. *Development* 1990, 635-644, 1990.
44. Hynes, R. O. and Destree, A. T. Relationships between fibronectin (LETS protein) and actin. *Cell* 1978, 875-86, 1978.
45. Lambert, Ch. A., Nusgens, B. V., and Lapierre, Ch. M. Mechano-sensing and mechano-reaction of soft connective tissue cells. *Adv Space Res* 1998, 1081-91, 1998.
46. Hynes, R. O. Cell adhesion: old and new questions. *Trends Cell Biol* 1999, M33-7, 1999.
47. Burridge, K. and Fath, K. Focal contacts: transmembrane links between the extracellular matrix and the cytoskeleton. *Bioessays* 1989, 104-8, 1989.
48. Curtis, A. and Wilkinson, C. New depths in cell behaviour: reactions of cells to nanotopography. *Biochem Soc Symp* 1999, 15-26, 1999.
49. Teixeira, A. I., Abrams, G. A., Bertics, P. J., Murphy, C. J., and Nealey, P. F. Epithelial contact guidance on well-defined micro- and nanostructured substrates. *J Cell Sci* 2003, 1881-92, 2003.
50. Teixeira, A. I., Nealey, P. F., and Murphy, C. J. Responses of human keratocytes to micro- and nanostructured substrates. *J Biomed Mater Res* 2004, 369-76, 2004.

51. Shirinsky, V. P., Antonov, A. S., Birukov, K. G., Sobolevsky, A. V., Romanov, Y. A., Kabaeva, N. V., Antonova, G. N., and Smirnov, V. N. Mechano-chemical control of human endothelium orientation and size. *J Cell Biol* 1989, 331-9, 1989 .